1080 *J. Chem. Eng. Data* **2007,** *52,* 1080−1085

Temperature and Pressure Dependence of the Viscosity of the Ionic Liquids 1-Hexyl-3-methylimidazolium Hexafluorophosphate and 1-Butyl-3-methylimidazolium Bis(trifluoromethylsulfonyl)imide

Kenneth R. Harris,*,† Mitsuhiro Kanakubo,†,‡ and Lawrence A. Woolf†

School of Physical, Environmental, and Mathematical Sciences, University College, University of New South Wales, Australian Defence Force Academy, Canberra, ACT 2600, Australia, and National Institute of Advanced Industrial Science and Technology (AIST), 4-2-1 Nigatake, Miyagino-ku, Sendai 983-8551, Japan

The viscosities of the ionic liquids 1-methyl-3-hexylimidazolium hexafluorophosphate, [HMIM]PF_6, and 1-butyl-3-methylimidazolium bis(trifluorosulfonyl)imide, [BMIM][Tf_2N], have been measured between (0 and 80) °C and at maximum pressures of 238 MPa ([HMIM]PF_6) and 300 MPa ([BMIM][Tf_2N]) at 75 °C with a falling-body viscometer. The overall uncertainty is estimated at ± 2 %. Modified Litovitz and Vogel−Fulcher−Tammann (VFT) equations are used to represent the temperature and pressure dependence. The Angell equation relating the strength factor D, the VFT parameter T_0, and the glass temperature T_g is confirmed. Densities between (0 and 90) °C at atmospheric pressure with an overall uncertainty estimated at ± 0.000 05 $g\cdot cm^{-3}$ are also reported.

Introduction

This work is the fourth in a series on the transport properties of ionic liquids at high pressure. Two have reported high-pressure viscosities for 1-butyl-3-methylimidazolium hexafluorophosphate ([BMIM]PF_6),[1] 1-methyl-3-octylimidazolium hexafluorophosphate ([OMIM]PF_6), and 1-methyl-3-octylimidazolium tetrafluoroborate ([OMIM]BF_4),[2] whereas the third has reported high-pressure ionic self-diffusion coefficients and conductivities for [BMIM]PF_6.[3] The first two studies showed how the falling-body method could be used successfully for these highly viscous fluids and how the Litovitz and Vogel−Fulcher−Tammann (VFT) equations for the temperature representation of the viscosity could be extended to high pressures. The third study allowed the first determination of ionic velocity cross correlation functions for molten salts at high pressures and the correlation of the pressure dependences of the transport properties using the Nernst−Einstein equation and the fractional form of the Stokes−Einstein equation. Here, we extend high-pressure viscosity measurements to two further ionic liquids, 1-methyl-3-hexylimidazolium hexafluorophosphate, [HMIM]PF_6, and 1-butyl-3-methylimidazolium bis(trifluoromethylsulfonyl)imide, [BMIM][Tf_2N]. We also report atmospheric pressure density measurements for these substances.

Experimental Section

Samples of [HMIM]PF_6 and [BMIM][Tf_2N], prepared and purified as described previously,[1,2,4] were sealed into glass ampoules and then opened and transferred to high-pressure cells inside a dry glove box just prior to use. The water contents of the samples were (17 and 19)$\cdot 10^{-6}$ mass fractions, respectively, as determined by Karl−Fischer titration, and the chloride contents of aqueous solutions in contact with the samples were less than the detection limit of $AgNO_3$ testing. The molar masses were taken as (312.232 and 419.362) $g\cdot mol^{-1}$, respectively.

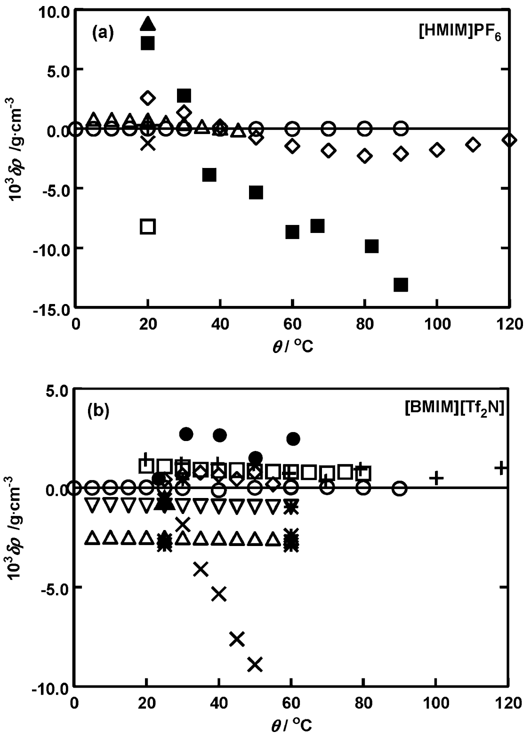

Figure 1. (a) Residuals (experimental − calculated values) for the fit of the experimental atmospheric pressure and literature densities for [HMIM]PF_6 to eq 4a as a function of temperature, θ. Open symbols and X and + refer to vibrating tube densimeters, and closed symbols refer to pycnometric and other techniques. Symbols: ○, this work; ◇, ref 5; X, ref 10; □, ref 11; +, (obscured: 20 °C, −0.3 $mg\cdot cm^{-3}$) ref 13; △, ref 14; ■, ref 9; ▲, ref 12. (b) Residuals (experimental − calculated values) for the fit of the experimental atmospheric pressure and literature densities for [BMIM][Tf_2N] to eq 4b as a function of temperature, θ. Symbols: ○, this work; ◇, ref 8; X, ref 10; □, ref 15; △, ref 18, Quill sample; ▽, ref 18, CA sample; *, ref 17; +, ref 19; ▲, (obscured: 25 °C, −0.6 $mg\cdot cm^{-3}$) ref 12; ●, ref 16.

We have determined the densities at atmospheric pressure using an Anton−Paar DMA5000 vibrating tube densimeter, with

---

* To whom correspondence should be addressed. Email: k.harris@adfa.edu.au.
† University of New South Wales, Australian Defence Force Academy.
‡ AIST.

10.1021/je700032n CCC: $37.00

Table 1. Density ρ of [HMIM]PF_6 from $\theta = (0 \text{ to } 90)$ °C

θ/°C	ρ/g·cm^{-3}	θ/°C	ρ/g·cm^{-3}
0.00	1.31339	40.00	1.28117
5.00	1.30933	50.00	1.27344
10.00	1.30529	60.00	1.26568
15.00	1.30126	60.00	1.26569
20.00	1.29724	70.00	1.25796
25.00	1.29322	80.00	1.25028
30.00	1.28921	90.00	1.24264

Table 2. Density ρ of [BMIM][Tf_2N] from $\theta = (0 \text{ to } 90)$ °C

θ/°C	ρ/g·cm^{-3}	θ/°C	ρ/g·cm^{-3}
	Sample 1		
0.00	1.46067	30.00	1.43186
5.00	1.45584	40.00	1.42234
10.00	1.45104	50.00	1.41287
15.00	1.44623	60.00	1.40348
20.00	1.44143	70.00	1.39415
20.00	1.44142	80.00	1.38488
25.00	1.43664	90.00	1.37567
	Sample 2		
25.00	1.43660	50.00	1.41285

an expanded uncertainty of 0.000 05 g·cm^{-3}. The built-in viscosity correction for this instrument has been confirmed for samples with known viscosities as high as 16 Pa·s.[2]

The experimental methods for the viscosity measurements have been given previously.[1,2] As before, two sinkers were employed, with nominal diameters of (6.3 and 6.0) mm for which calibrations cover the viscosity range (0.3 to 2875) mPa·s. Combination of the uncertainties in replicate measurements (±1 %), the calibration (±1 %), and the calibrant viscosities (the uncertainty for the most viscous, Cannon N1000, is ±0.38 % for the temperatures employed) in quadrature yields an expanded uncertainty of ±2 %.

Falling-body viscosity measurements require an estimate for the density for the buoyancy factor $(1 - \rho/\rho_s)$ in the primary working equation

$$\eta(p,T) = \frac{t(1 - \rho/\rho_s)}{A[(1 + 2\alpha(T - T_{ref}))][1 - 2\beta(p - p_{ref})/3]} \qquad (1)$$

where ρ/ρ_s is the ratio of the density ρ for the fluid at the temperature T and pressure p of the measurement to that of the sinker ρ_s. (The other quantities in eq 1 are the calibration constant, A, the fall time, t, and α and β, the coefficients of expansion and compressibility of the sinker and viscometer tube material, 316 stainless steel, at (T_{ref}, p_{ref}).) ρ_s is 7.285 g·cm^{-3} at 25 °C and 0.1 MPa, so for a fluid such as [HMIM]PF_6 with a density of 1.2932 g·cm^{-3} under the same conditions, the density need only be known to better than 0.5 % to give 0.1 % accuracy in the buoyancy factor. There appear to be no *pVT* data in the literature for [HMIM]PF_6 that we could use for this purpose: those of Gardas et al.[5] and of Tomida et al.[6] extend to only (10 and 20) MPa, respectively. Consequently, we have assumed that the p,T dependence of the compressibility of [HMIM]PF_6 is similar to those of [BMIM]PF_6 and [OMIM]PF_6 and used bulk secant moduli (K) calculated[1,2] from the *pVT* data of Gu and Brennecke[7] to estimate the densities at high pressure. These extend to approximately 200 MPa at (25 and 50) °C for both substances. K is defined in terms of the pressure and molar volume, V

$$K = V_0(p - p_0)/(V_0 - V) \qquad (2)$$

where V_0 is the molar volume at a given temperature obtained from our own atmospheric pressure (p_0) densities. K was expressed by the Hayward-type equation

$$K = (\alpha_{00} + \alpha_{10}/T) + (\alpha_{01} + \alpha_{11}/T)p \qquad (3)$$

and the fitted sets of α_{ij} coefficients for [BMIM]PF_6 and [OMIM]PF_6 are given in our previous work.[1,2] It made no difference to the calculated viscosities which set of α_{ij} coefficients were used for [HMIM]PF_6. The viscosity tables

Table 3. Viscosity η of [HMIM]PF_6 from $\theta = (0 \text{ to } 80)$ °C and $p = (0.1 \text{ to } 238)$ MPa (6.0 mm Sinker)

θ/°C	t/s	p/MPa	V/cm^3·mol^{-1}	ρ/g·cm^{-3}	η/mPa·s	Re[a]	θ/°C	t/s	p/MPa	V/cm^3·mol^{-1}	ρ/g·cm^{-3}	η/mPa·s	Re[a]
0.00	11830	0.1	237.73	1.3134	3924	0.0002	50.00	355.4	7.6	244.32	1.2780	118.3	0.21
5.00	7317	0.1	238.47	1.3093	2428	0.0005	50.00	486.4	25.8	242.38	1.2882	161.7	0.11
10.00	4717	0.1	239.21	1.3053	1566	0.0012	50.00	654.6	50.6	240.06	1.3007	217.1	0.063
10.00	4715	0.1	239.21	1.3053	1565	0.0012	50.00	878.0	76.0	237.99	1.3119	290.7	0.036
15.00	3120	0.1	239.95	1.3013	1036	0.0028	50.00	1162	100.9	236.23	1.3218	384.0	0.021
15.00	3117	0.1	239.95	1.3013	1035	0.0028	50.00	1527	125.8	234.66	1.3306	503.9	0.012
20.00	2122	0.1	240.69	1.2972	705.1	0.0060	50.00	1987	150.1	233.30	1.3383	655.0	0.0072
20.00	2122	0.1	240.69	1.2972	705.1	0.0060	50.00	2582	174.8	232.06	1.3455	850.1	0.0043
25.00	1494	0.1	241.44	1.2932	496.5	0.012	60.00	225.4	0.1	246.69	1.2657	75.2	0.52
25.00	1494	0.1	241.44	1.2932	496.4	0.012	60.00	223.1	0.1	246.69	1.2657	74.4	0.53
25.00	2066	22.0	239.28	1.3049	685.3	0.0064	60.00	223.1	0.1	246.69	1.2657	74.4	0.53
25.00	2771	42.1	237.53	1.3145	917.7	0.0036	60.00	356.6	40.5	242.28	1.2887	118.5	0.21
25.00	3597	60.3	236.10	1.3225	1190	0.0021	60.00	552.0	80.8	238.83	1.3075	182.8	0.090
25.00	4760	80.3	234.68	1.3305	1572	0.0012	60.00	834.4	120.8	236.06	1.3227	275.7	0.040
25.00	6255	100.1	233.40	1.3378	2064	0.0007	60.00	1240	160.6	233.79	1.3355	408.7	0.018
30.00	1073	0.1	242.19	1.2892	356.9	0.023	60.00	1820	200.1	231.90	1.3464	598.9	0.0086
30.00	1073	0.1	242.19	1.2892	356.8	0.023	70.00	148.8	0.1	248.21	1.2580	49.7	1.2
40.00	591.8	0.1	243.71	1.2812	197.0	0.076	70.00	148.9	0.1	248.21	1.2580	49.7	1.2
40.00	591.9	0.1	243.71	1.2812	197.0	0.076	75.00	123.8	0.1	248.97	1.2541	41.3	1.7
40.00	592.8	0.4	243.67	1.2814	197.3	0.076	75.00	125.6	0.8	248.88	1.2546	41.9	1.6
40.00	833.0	25.7	241.03	1.2954	276.7	0.039	75.00	191.4	40.7	244.25	1.2783	63.7	0.73
40.00	1152	50.8	238.77	1.3077	381.8	0.021	75.00	284.1	80.8	240.63	1.2976	94.2	0.34
40.00	1577	76.0	236.80	1.3185	521.9	0.011	75.00	412.6	120.7	237.73	1.3134	136.4	0.16
40.00	2144	101.4	235.07	1.3283	708.3	0.0061	75.00	590.5	160.6	235.35	1.3267	194.8	0.081
40.00	2847	125.2	233.62	1.3365	939.3	0.0035	75.00	833.3	200.2	233.38	1.3379	274.5	0.041
40.00	3806	150.0	232.28	1.3442	1254	0.0020	75.00	1149	238.5	231.76	1.3472	378.0	0.022
50.00	357.9	0.1	245.19	1.2734	119.2	0.21	80.00	104.3	0.1	249.73	1.2509	34.8	2.4
50.00	351.3	0.1	245.19	1.2734	117.0	0.21	80.00	104.3	0.1	249.73	1.2509	34.8	2.4
50.00	351.3	0.1	245.19	1.2734	117.0	0.21							

[a] Reynolds number for annular flow: $Re = 2r_1^2\rho v/((r_2 - r_1)\eta)$ where v is the terminal velocity of the sinker and r_1 and r_2 are the radii of the sinker and tube, respectively.

Table 4. Viscosity η of [BMIM][Tf$_2$N] from θ = (0 to 80) °C and p = (0.1 to 300) MPa

θ/°C	t/s	p/MPa	V/cm^3·mol^{-1}	ρ/g·cm^{-3}	η/mPa·s	Re^a
			6.0 mm sinker			
0.00	592.2	0.1	287.10	1.4607	191.6	0.089
0.00	591.2	0.1	287.10	1.4607	191.3	0.089
5.00	433.8	0.1	288.05	1.4558	140.4	0.17
5.00	433.8	0.1	288.05	1.4558	140.4	0.17
10.00	327.7	0.1	289.01	1.4510	106.1	0.29
10.00	454.5	24.3	285.76	1.4674	146.8	0.15
10.00	638.8	49.9	282.81	1.4827	205.8	0.078
10.00	872.3	74.1	280.44	1.4952	280.3	0.042
15.00	251.6	0.1	289.97	1.4462	81.6	0.49
15.00	251.7	0.1	289.97	1.4462	81.6	0.49
20.00	196.7	0.1	290.93	1.4414	63.8	0.79
20.00	196.9	0.1	290.93	1.4414	63.9	0.79
25.00	157.2	0.1	291.90	1.4366	51.0	1.2
25.00	157.4	0.1	291.90	1.4366	51.1	1.2
25.00	156.9	0.1	291.90	1.4366	50.9	1.2
25.00	210.5	24.3	288.46	1.4537	68.1	0.70
25.00	281.8	49.3	285.37	1.4694	90.9	0.40
25.00	385.4	76.9	282.41	1.4848	124.0	0.22
25.00	502.9	101.5	280.11	1.4970	161.5	0.13
25.00	656.3	126.4	278.03	1.5082	210.3	0.076
25.00	842.1	150.2	276.24	1.5179	269.4	0.046
30.00	127.9	0.1	292.88	1.4319	41.5	1.9
30.00	127.9	0.1	292.88	1.4319	41.5	1.9
40.00	87.61	0.1	294.84	1.4223	28.5	3.9
40.00	87.58	0.1	294.84	1.4223	28.5	3.9
50.00	63.03	0.1	296.82	1.4129	20.5	7.6
50.00	63.02	0.1	296.82	1.4129	20.5	7.6
50.00	82.78	26.4	292.87	1.4317	26.9	4.5
50.00	107.0	52.0	289.38	1.4490	34.6	2.7
50.00	129.0	75.0	286.52	1.4635	41.6	1.9
50.00	167.6	101.6	283.48	1.4792	53.9	1.1
50.00	260.9	152.8	278.34	1.5065	83.6	0.48
50.00	386.0	200.3	274.24	1.5290	123.2	0.22
50.00	474.8	226.0	272.25	1.5402	151.2	0.15
50.00	576.2	249.6	270.53	1.5500	183.2	0.10
			6.3 mm sinker			
50.00	736.2	0.1	296.82	1.4129	20.6	1.60
50.00	737.3	0.1	296.82	1.4129	20.7	1.6
50.00	734.6	0.1	296.82	1.4129	20.6	1.6
50.00	1045.5	35.6	291.58	1.4381	29.2	0.81
50.00	1247.8	53.9	289.14	1.4502	34.8	0.58
50.00	1443.9	69.8	287.14	1.4603	40.2	0.43
50.00	1963.9	103.6	283.26	1.4803	54.4	0.24
50.00	2324.6	123.6	281.17	1.4913	64.3	0.17
60.00	549.7	0.1	298.80	1.4035	15.43	2.8
60.00	551.3	0.1	298.80	1.4035	15.48	2.8
70.00	426.6	0.1	300.80	1.3942	11.99	4.7
70.00	425.8	0.1	300.80	1.3942	11.97	4.7
75.00	377.8	0.1	301.80	1.3895	10.64	5.9
75.00	381.0	0.1	301.80	1.3895	10.71	5.9
75.00	381.7	0.8	301.80	1.3895	10.73	5.8
75.00	477.6	25.7	297.74	1.4084	13.4	3.8
75.00	587.1	50.7	293.97	1.4264	16.4	2.5
75.00	715.7	75.6	290.39	1.4440	19.9	1.7
75.00	869.4	100.9	286.93	1.4614	24.2	1.2
75.00	1045.1	125.5	283.71	1.4780	29.0	0.84
75.00	1251.3	150.6	280.58	1.4945	34.6	0.59
75.00	1486.0	175.4	277.62	1.5104	40.9	0.43
75.00	1488.8	175.6	277.60	1.5105	41.0	0.43
75.00	1767.0	200.6	274.74	1.5262	48.6	0.31
75.00	2094.8	225.4	272.02	1.5415	57.4	0.22
75.00	2462.3	249.7	269.47	1.5561	67.3	0.16
75.00	2897.9	274.5	266.97	1.5707	79.0	0.12
75.00	3405.8	298.9	264.61	1.5847	92.6	0.09
80.00	338.8	0.1	302.81	1.3849	9.53	7.4
80.00	338.6	0.1	302.81	1.3849	9.53	7.4

[a] Reynolds number for annular flow: $\mathrm{Re} = 2r_1^2\rho v/((r_2 - r_1)\eta)$ where v is the terminal velocity of the sinker and r_1 and r_2 are the radii of the sinker and tube, respectively.

presented below give sufficient detail for the viscosities to be recalculated when more extensive *pVT* data become available.

For [BMIM][Tf$_2$N], the situation is a little better as Gomez de Azevedo et al.[8] have determined densities between (25 and 55) °C, though to only 59.1 MPa. The data have been fitted to eq 3 with a standard uncertainty of fit of 0.02 %, with coefficients α_{00} = 1521.44 MPa, α_{10} = 114.760 GPa·K, α_{01} = −22.0546, and a_{11} = 8345.90 K. The uncertainties in the densities estimated from these methods should be less than 0.5 %.

Results and Discussion

The density results at atmospheric pressure are presented in Tables 1 and 2; they can be represented by the polynomials

$$\rho([\mathrm{HMIM}]\mathrm{PF}_6)/\mathrm{g\cdot cm^{-3}} = 1.31341 - 8.16298\cdot 10^{-4}\,(\theta/°\mathrm{C}) + 3.39128\cdot 10^{-7}\,(\theta/°\mathrm{C})^2 \quad (4a)$$

$$\rho([\mathrm{BMIM}][\mathrm{Tf_2N}])/\mathrm{g\cdot cm^{-3}} = 1.46070 - 9.70080\cdot 10^{-4}\,(\theta/°\mathrm{C}) + 2.78909\cdot 10^{-7}\,(\theta/°\mathrm{C})^2 \quad (4b)$$

where θ is the Celsius temperature, with standard uncertainties of fit of (± 0.000 04 and ± 0.000 02) g·cm^{-3}, respectively. Some checkpoints are also included for a second aliquot of [BMIM][Tf$_2$N] from a different sealed ampoule, determined 12 months after the first set: the agreement is satisfactory. Figure 1a shows deviations of literature density data for [HMIM]PF$_6$[5,9−14] from the values calculated with eq 4a. There is very good agreement with the vibrating tube densimeter results of Gardas et al.,[5] Dyzuba and Bartsch,[10] Letcher and Reddy,[13] and Pereiro et al.[14] None of these works mention the application of a viscosity correction, though Letcher and Reddy did employ an Anton−Paar DMA5000 densimeter. The pycnometric results of Seddon et al.[9] deviate systematically with changing temperature in this case. Figure 1b shows deviations of literature density data for [BMIM][Tf$_2$N][8,10,12,15−19] from the values calculated with eq 4b. Of the vibrating tube work,[8,10,15,17−18] only the paper of Troncoso et al.[18] mentions the application of a viscosity correction (again for an Anton−Paar DMA5000 densimeter), though Canongia Lopes et al.[17] also employed the same instrument. Nevertheless, there is good agreement between the data sets, particularly with regard to the temperature dependence, with the single exception of those of Dyzuba and

Table 5. Coefficients of Best Fit for Equations 5 and 6

	coefficients and standard uncertainties	
	[HMIM]PF$_6$	[BMIM][Tf$_2$N]
Litovitz, eq 5		
ln(A/mPa·s)	−0.5224 ± 0.011	−0.3254 ± 0.009
$B/R\cdot 10^{-6}$/K^3	178.671 ± 0.32	113.205 ± 0.26
standard uncertainty of fit/%	1.3	1.2
VFT, eq 6		
ln(A'/mPa·s)	−3.0557 ± 0.047	−1.8114 ± 0.020
B'/K	1262.8 ± 14	766.28 ± 5.6
T_0/K	161.794 ± 0.79	164.739 ± 0.51
D^a	7.81	4.65
standard uncertainty of fit/%	1.2	0.3

[a] Angell strength factor (B'/T_0).

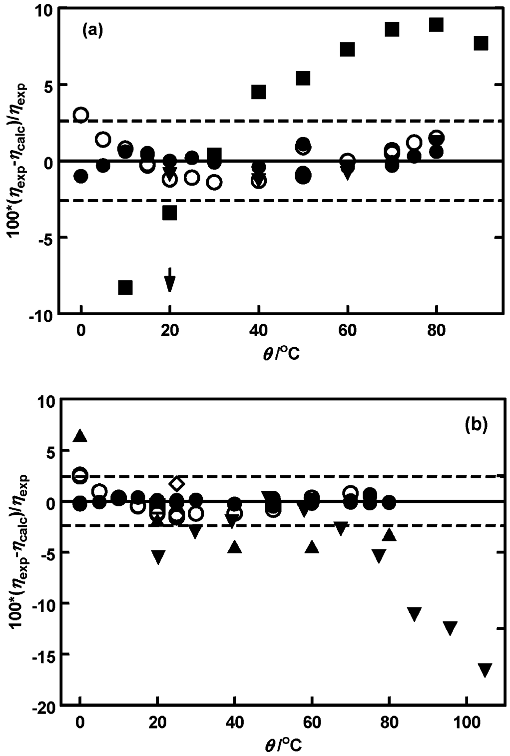

Figure 2. (a) Residuals (experimental − calculated values) for the fit of the experimental atmospheric pressure and literature viscosities for [HMIM]-PF_6 to eqs 5 and 6 as a function of temperature, θ. The dashed lines represent the expanded uncertainty of fit ($k = 2$) or 95 % confidence limits for the Litovitz equation. Symbols: ○, this work, Litovitz eq 5; ●, this work, VFT eq 6; ■, ref 9; ↓, ref 20 (20 °C, −41 %); ▼, ref 6, all Litovitz eq 5. (b) Residuals (experimental − calculated values) for the fit of the experimental atmospheric pressure and literature viscosities for [BMIM][Tf_2N] to eqs 5 and 6 as a function of temperature, θ. The dashed lines represent the expanded uncertainty of fit ($k = 2$) or 95 % confidence limits for the Litovitz equation. Symbols: ○, this work, Litovitz eq 5; ●, this work, VFT eq 6; □, (obscured: 20 °C, −0.5 %) ref 22; ◇, ref 23; ▲, ref 21; ▼, ref 19, all VFT eq 6.

Table 6. Coefficients of Best Fit for Equations 7, 8, and 9

	coefficients and standard uncertainties	
	[HMIM]PF_6	[BMIM][Tf_2N]
	ML, eq 7	
a	−0.51513 ± 0.0081	−0.31943 ± 0.0079
$b\cdot10^3/\mathrm{MPa}^{-1}$	3.268 ± 0.17	2.512 ± 0.11
$c\cdot10^{-6}/\mathrm{K}^3$	178.404 ± 0.24	113.024 ± 0.23
$d\cdot10^{-6}/(\mathrm{K}^3\cdot\mathrm{MPa}^{-1})$	0.30742 ± 0.0047	0.25008 ± 0.0033
$e/(\mathrm{K}^3\cdot\mathrm{MPa}^{-2})$	−217.1 ± 15	−169.07 ± 9.2
standard uncertainty of fit/%	1.0	1.1
	MVFT1, eq 8	
a'	−2.9817 ± 0.040	−1.7696 ± 0.034
$b'\cdot10^3/\mathrm{MPa}^{-1}$	−1.408 ± 0.134	−0.9613 ± 0.090
c'/K	1241.0 ± 12	754.98 ± 9.6
$d'/(\mathrm{K}\cdot\mathrm{MPa}^{-1})$	2.2097 ± 0.020	1.7102 ± 0.017
$e'\cdot10^5/(\mathrm{K}\cdot\mathrm{MPa}^{-2})$	−99.76 ± 3.9	−74.85 ± 2.3
T_0/K	163.023 ± 0.66	165.715 ± 0.88
standard uncertainty of fit/%	0.5	0.8
	MVFT2, eq 9	
a''	−3.1203 ± 0.042	−1.9381 ± 0.051
$b''\cdot10^3/\mathrm{MPa}^{-1}$	3.1928 ± 0.090	2.7072 ± 0.088
D	7.986 ± 0.11	4.995 ± 0.13
x/K	160.609 ± 0.71	161.14 ± 1.3
$y\cdot10^2/(\mathrm{K}\cdot\mathrm{MPa}^{-1})$	9.1996 ± 0.085	11.196 ± 0.12
$z\cdot10^5/(\mathrm{K}\cdot\mathrm{MPa}^{-2})$	−9.234 ± 0.21	−11.126 ± 0.26
standard uncertainty of fit/%	0.5	0.9

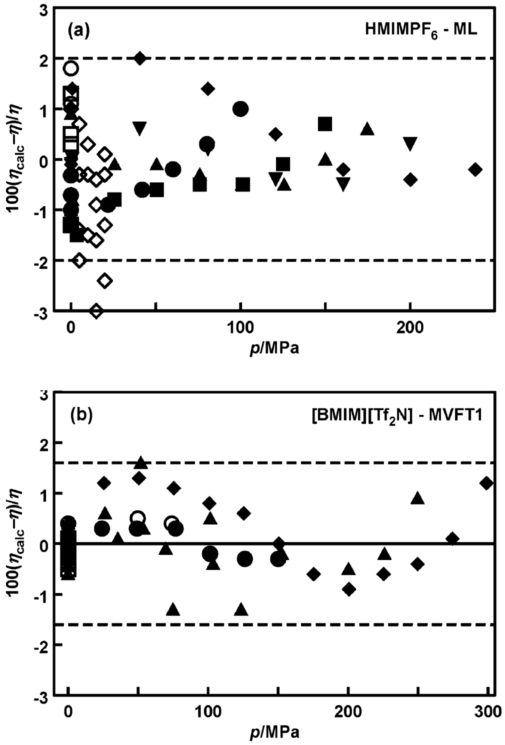

Figure 3. (a) Residuals (experimental − calculated values) for the fit of the experimental atmospheric pressure and literature viscosities for [HMIM]-PF_6 to eq 7 (modified Litovitz) as a function of pressure, p. The dashed lines represent the expanded uncertainty of fit ($k = 2$) or 95 % confidence limits for the fit. Symbols: ○, (5−20) °C; ●, 25 °C; □, (30, 70, 80) °C; ■, 40 °C; ▲, 50 °C; ▼, 60 °C; ◆, 75 °C, this work; ◇, (20, 40, 60, 80) °C, (0.1−20) MPa, ref 6. (b) Residuals (experimental − calculated values) for the fit of the experimental atmospheric pressure and literature viscosities for [BMIM][Tf_2N] to eq 8 (modified VFT) as a function of pressure, p. Symbols: ○, (5−20) °C; ●, 25 °C; □, (30, 70, 80) °C; ■, 40 °C; ▲, 50 °C; ▼, 60 °C; ♦, 75 °C.

Bartsch,[10] which trend lower at higher temperatures. Similar behavior was observed for [BMIM]PF_6.[1] If this data set is excepted, then of the ionic liquids whose densities we have determined, [BMIM][Tf_2N] shows the smallest differences between data sets from different laboratories, samples, and types of instrument.

Tables 3 and 4 list the high-pressure viscosity results for [HMIM]PF_6 and [BMIM][Tf_2N], respectively. As in our earlier studies,[1,2] the data at atmospheric pressure were fitted to the Litovitz equation

$$\eta = A\exp(B/RT^3) \tag{5}$$

and the Vogel−Fulcher−Tammann (VFT) equation

$$\eta = A'\exp(B'/(T - T_0)) \tag{6}$$

with coefficients being given in Table 5.

Figures 2a and 2b show the deviations of our results and the literature data[6,9,19−23] from these equations. When expanded to a larger scale, the residual plots show some systematic trends at the temperature extremes, but these are within the overall experimental uncertainty. The viscosities of the Seddon group[9] show systematic deviations with temperature for [HMIM]PF_6: this behavior is similar to that observed for their results for [OMIM]BF_4 and [OMIM]PF_6,[2] though the temperature at which their data intersect ours is lower for this example. Their water concentration was $28\cdot10^{-6}$ mass fraction, comparable to ours, so water is unlikely to be the cause of the differences observed. They used a cone and plate viscometer. On the other hand, the

Table 7. Test of the Angell Relationship between D, T_0, and T_g

	$[BMIM]PF_6$[a]	$[HMIM]PF_6$	$[OMIM]PF_6$[b]	$[BMIM][Tf_2N]$
Parameters from VFT, eq 6				
T_0/K	161.8	161.8	158.0	164.7
D	6.96	7.81	8.91	4.65
T_g/K	197.1	195.1[c]	191.2	186.3[d]
T_g/T_0	1.22	1.21	1.21	1.13
T_g/T_0 from eq 10	1.18	1.20	1.23	1.12
Parameters from MVFT2, eq 9				
$T_0(=x)$/K	156.2	160.6	158.2	160.6
D	7.80	7.99	8.87	5.00
T_g/T_0	1.26	1.22	1.21	1.16
T_g/T_0 from eq 10	1.20	1.20	1.23	1.13

[a] Ref 1. [b] Ref 2. [c] Ref 25. [d] Mean of values given in refs 10 and 26 (186 K) and ref 16 (187 K): the value of 169.2 K given in ref 25 appears to be too low.

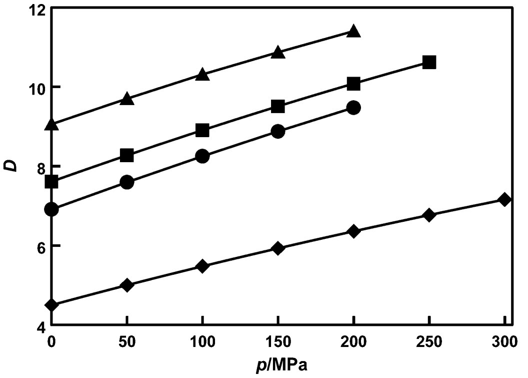

Figure 4. Pressure dependence of the Angell strength parameter D, obtained from the parameters of eq 8. Symbols: ■, $[HMIM]PF_6$; ▲, $[OMIM]PF_6$, from ref 2; ●, $[BMIM]PF_6$, from ref 1; ◆, $[BMIM][Tf_2N]$.

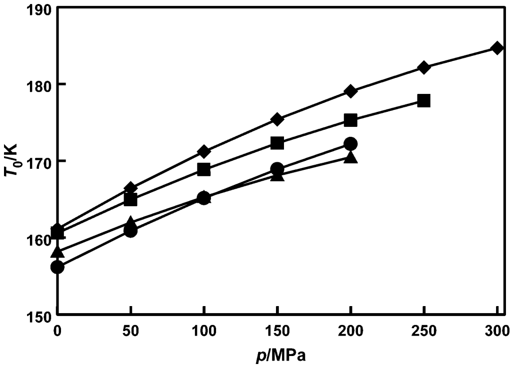

Figure 5. Pressure dependence of the VFT parameter T_0, obtained from the parameters of eq 9. Symbols: same as those for Figure 4.

very recent results of Tomida et al.,[6] obtained by the rolling-ball method at pressures up to 20 MPa from (20 to 80) °C with a sample containing $40 \cdot 10^{-6}$ mass fraction of water, are in excellent agreement with ours. The single point at 20 °C of Fitchett et al.,[20] obtained with a cross-arm capillary viscometer, is some 40 % below our correlation. For $[BMIM][Tf_2N]$, the careful capillary measurements of Widegren et al.[22] at 20 °C on a sample containing $10 \cdot 10^{-6}$ mass fraction of water are in excellent agreement with our measurements. So also is the point at 25 °C of François et al.[23] performed with the unusual technique of capillary electrophoresis, though the sample had a high water content, $235 \cdot 10^{-6}$ mass fraction. The results of Tokuda et al.[21] (water content $<40 \cdot 10^{-6}$ mass fraction), also determined with a cone-plate viscometer, and those of Jacquemin et al.[19] (water content $<50 \cdot 10^{-6}$ mass fraction), determined with a Couette (rotating cylinder) viscometer, claimed to have an uncertainty of 1 %; both lie systematically lower than ours.

As for other ionic liquids,[1,2] we have used the modified Litovitz (ML) and VFT (MVFT1 and MVFT2) equations to fit the data set as a whole:

$$\eta = \exp(a + bp + (c + dp + ep^2)/T^3) \tag{7}$$

$$\eta = \exp(a' + b'p + (c' + d'p + e'p^2)/(T - T_0)) \tag{8}$$

$$\eta = \exp(a'' + b''p + DT_0(p)/(T - T_0))$$

$$T_0(p) = x + yp + zp^2 \tag{9}$$

The Angell strength parameter D ($\equiv B'/T_0$ in eq 6) is large for "strong" liquids where the viscosity approaches an Arrhenius (Andrade) temperature dependence and is small for "fragile" liquids.[24] The MVFT1 form has a pressure-dependent strength factor D [$=(c' + d'p + e'p^2)/T_0$], whereas the MVFT2 form has a pressure-dependent T_0. The coefficients for these fits are given in Table 6. Figure 3 shows residuals for two of the six fits, ML for $[HMIM]PF_6$ and MVFT1 for $[BMIM][Tf_2N]$. The moderate-pressure (20 MPa maximum) results of Tomida et al.[6] for $[HMIM]PF_6$ have an average deviation of (1.2 and 0.8) %, respectively, from values calculated from eqs 7 and 8.

The D value for $[HMIM]PF_6$ determined from the atmospheric pressure values is 7.81, which lies between the values for $[BMIM]PF_6$ and $[OMIM]PF_6$, 7.0 and 8.91, respectively. D for the more fragile $[BMIM][Tf_2N]$ is 4.65. Angell[24] has suggested the following relationship between D, T_0, and the glass temperature T_g, based on the scaling of the (coexistence line) viscosities of a wide range of liquids in the range $0 < (T_g/T_0) < 1$, with the assumption of a common single viscosity value (η_g) at T_g. Thus

$$T_g/T_0 = 1 + D/(2.303 \log(\eta_g/\eta_0)) \tag{10}$$

η_0 is A' of the VFT equation (eq 5). Angell found $\log(\eta_g/\eta_0)$ empirically to be about 17. The values of D and T_0 derived from VFT and MVFT2 and experimental T_g values from the literature[10,16,25,26] are found to be generally consistent with Angell's relationship (Table 7). Figures 4 and 5 show the pressure dependences of D and T_0, with values for $[BMIM]PF_6$ and $[OMIM]PF_6$ also being given for comparison with $[HMIM]PF_6$.

Literature Cited

(1) Harris, K. R.; Woolf, L. A.; Kanakubo, M. Temperature and pressure dependence of the viscosity of the ionic liquid 1-butyl-3-methylimidazolium hexafluorophosphate. *J. Chem. Eng. Data* **2005**, *50*, 1777−1782.

(2) Harris, K. R.; Kanakubo, M.; Woolf, L. A. Temperature and pressure dependence of the viscosity of the ionic liquid 1-methyl-3-octylimidazolium hexafluorophosphate and 1-methyl-3-octylimidazolium tetrafluoroborate. *J. Chem. Eng. Data* **2006**, *51*, 1161−1167.

(3) Kanakubo, M.; Harris, K. R.; Tsuchihashi, N.; Ibuki, K.; Ueno, M. Effect of pressure on transport properties of the ionic liquid 1-butyl-3-methylimidazolium hexafluorophosphate. *J. Phys. Chem. B* **2007**, *111*, 2062−2069.

(4) Umecky, T.; Kanakubo, M.; Ikushima, Y. Self-diffusion coefficients of 1-butyl-3-methylimidazolium hexafluorophosphate with pulsed-field gradient spin-echo NMR technique. *Fluid Phase Equilib.* **2005**, *228−229*, 329−333.

(5) Gardas, R. L.; Freire, M. G.; Carvalho, P. J.; Marrucho, I. M.; Fonseca, I. M. A.; Ferreira, A. G. M.; Coutinho, J. A. P. High-pressure densities and derived thermodynamic properties of imidazolium-based ionic liquids. *J. Chem. Eng. Data* **2007**, *52*, 80−88.

(6) Tomida, D.; Kumagai, A.; Kenmochi, S.; Qiao, K.; Yokoyama, C. Viscosity of 1-hexyl-3-imidazolium hexafluorophosphate and 1-octyl-

3-imidazolium hexafluorophosphate at high pressure. *J. Chem. Eng. Data* **2007**, *52*, 577−579.

(7) Gu, Z.; Brennecke, J. F. Volume expansivities and isothermal compressibilities of imidazolium and pyridinium-based ionic liquids. *J. Chem. Eng. Data* **2002**, *47*, 339−345.

(8) Gomes de Azevedo, R.; Esperança, J. M. S. S.; Szydlowski, J.; Visak, Z. P.; Pires, P. F.; Guedes, H. J. R.; Rebelo, L. P. N. Thermophysical and thermodynamic properties of ionic liquids over an extended pressure range: [bmim][NTf_2] and [hmim][NTf_2]. *J. Chem. Thermodyn.* **2005**, *37*, 888−899.

(9) Seddon, K. R.; Stark, A.; Torres, M.-J. Viscosity and density of 1-alkyl-3-methylimidazolium ionic liquids. In *Clean Solvents: Alternative Media for Chemical Reactions and Processing*; Abraham, M. A., Moens, L., Eds.; ACS Symposium Series 819; American Chemical Society: Washington, DC, 2002; p 34−49.

(10) Dzyuba, S. V.; Bartsch, R. A. Influence of structural variations in 1-alkyl(aralkyl)-3-methylimidazolium hexafluorophosphates and bis-(trifluoromethylsulfonyl)imides on physical properties of the ionic liquids. *ChemPhysChem* **2002**, *3*, 161−166.

(11) Vidal, S. T. M.; Correia, M. J. N.; Marques, M. M.; Ismael, M. R.; Reis, M. T. A. Studies on the use of ionic liquids as potential extractants of phenolic compounds and metal ions. *Sep. Sci. Technol.* **2004**, *39*, 2155−2169.

(12) Lee, S. H.; Lee, S. B. The Hildebrand solubility parameters, cohesive energy densities and internal energies of 1-alkyl-3-methylimidazolium-based room temperature ionic liquids. *Chem. Commun.* **2005**, 3469−3471.

(13) Letcher, T. M.; Reddy, P. Ternary (liquid+ liquid) equilibria for mixtures of 1-hexyl-3-methylimidazolium (tetrafluoroborate or hexafluorophosphate) + benzene + an alkane at $T = 298.2$ K and $p = 0.1$ MPa. *J. Chem. Thermodyn*. **2005**, *37*, 415−421.

(14) Pereiro, A. B.; Tojo, E.; Rodríguez, A.; Canosa, J.; Tojo, J. Properties of ionic liquid $HMIMPF_6$ with carbonates, ketones and alkyl acetates. *J. Chem. Thermodyn*. **2006**, *38*, 651−661.

(15) Krummen, M.; Wasserscheid, P.; Gmehling, J. Measurement of activity coefficients at infinite dilution in ionic liquids using the dilutor technique. *J. Chem. Eng. Data* **2002**, *47*, 1411−1417.

(16) Fredlake, C. P.; Crosthwaite, J. M.; Hert, D. G.; Aki, S. N. V. K.; Brennecke, J. F. Thermophysical properties of imidazolium-based ionic liquids. *J. Chem. Eng. Data* **2004**, *49*, 954−964.

(17) Canongia Lopes, J. N.; Cordeiro, T. C.; Esperança, J. M. S. S.; Guedes, H. J. R.; Huq, S.; Rebelo, L. P. N.; Seddon, K. R. Deviations from ideality in mixtures of two ionic liquids containing a common ion. *J. Phys. Chem. B* **2005**, *109*, 3519−3525.

(18) Troncoso, J.; Cerdeiriña, C. A.; Sanmamed, Y. A.; Romani, L.; Rebelo, L. P. N. Thermodynamic properties of imidazolium-based ionic liquids: densities, heat capacities, and enthalpies of fusion of [bmim]-[PF_6] and [bmim][NTf_2]. *J. Chem. Eng. Data* **2006**, *51*, 1856−1859.

(19) Jacquemin, J.; Husson, P.; Padua, A. A. H.; Majer, V. Density and viscosity of several pure and water-saturated ionic liquids. *Green Chem.* **2006**, *8*, 172−180.

(20) Fitchett, B. D.; Knepp, T. N.; Conboy, J. C. 1-Alkyl-3-methylimidazolium bis(perfluoroalkylsulfonyl)imide water-immiscible ionic liquids. *J. Electrochem. Soc.* **2004**, *151*, E219−E215.

(21) Tokuda, H.; Hayamizu, K.; Ishii, K.; Susan, M. A. B. H.; Watanabe, M. Physicochemical properties and structures of room temperature ionic liquids. 1. Variation of anionic species. *J. Phys. Chem. B* **2004**, *108*, 16593−16600.

(22) Widegren, J. A.; Laesecke, A.; Magee, J. W. The effect of dissolved water on the viscosities of hydrophobic room-temperature ionic liquids. *Chem. Commun*. **2005**, 1610−1612.

(23) François, Y.; Zhang, K.; Varenne, A.; Gareil, P. New integrated measurement protocol using capillary electrophoresis instrumentation for the determination of viscosity, conductivity and absorbance of ionic liquid−molecular solvent mixtures. *Anal. Chim. Acta* **2006**, *562*, 164−170.

(24) Angell, C. A. Formation of glasses from liquids and biopolymers. *Science* **1995**, *267*, 1924−1935.

(25) Huddleston, J. G.; Visser, A. E.; Reichert, W. M.; Willauer, H. D.; Broker, G. A.; Rogers, R. D. Characterization and comparison of hydrophilic and hydrophobic room temperature ionic liquids incorporating the imidazolium cation. *Green Chem*. **2001**, *3*, 156−164.

(26) Tokuda, H.; Hayamizu, K.; Ishii, K.; Susan, M. A. B. H.; Watanabe, M. Physicochemical properties and structures of room temperature ionic liquids. 2. Variation of alkyl chain length in imidazolium cation. *J. Phys. Chem. B* **2005**, *109*, 6103−6110.

Received for review January 23, 2007. Accepted March 7, 2007. M.K. would like to thank the Japan Society for the Promotion of Science and the University of New South Wales for their financial support and the Australian Academy of Science for its administration of the JSPS Fellowship through the International Science Linkages Programme.

JE700032N